Soils and Rocks
www.soilsandrocks.com
An International Journal of Geotechnical and Geoenvironmental Engineering
ISSN 1980-9743
ISSN-e 2675-5475

Lining forces in tunnel interaction problems

António M. G. Pedro[1#], José C. D. Grazina[2], Jorge N. V. Almeida e Sousa[2]

Article

Keywords
Twin tunnels
Lining forces
Numerical modelling

Abstract

In big cities the construction of new tunnels in close proximity to existing ones is unavoidable given the densely and growing occupation of the subsoil. The interaction between tunnels in such conditions is well identified in the literature and has been thoroughly investigated in the past. However, most of those studies are focused on the effect of the ground conditions and relative position between tunnels on the ground movements and often disregard the impact induced by the second excavation on the lining forces of both tunnels. To provide further insight into this subject a numerical study of the sequential excavation of side-by-side twin tunnels is presented in this paper. The study also assesses the influence of parameters that have not been covered in the previous studies, namely the stiffness of the lining and the initial stress conditions. The results confirm that significant interaction occurs when the tunnels are spaced less than one diameter, where a considerable increase on both hoop forces and bending moments, particularly on the lining of the existing tunnel, is observed after the second excavation. For a spacing higher than two diameters the interaction between tunnels is almost negligible. The magnitude of the lining forces and of the interaction effects are also dependent of the stiffness of the linings and of the initial stress conditions.

1. Introduction

Having an efficient and sustainable transportation network is a fundamental condition for the development of a city (Admiraal & Cornaro, 2016). Given the increasing occupation at ground surface and the growing environment awareness the most frequently adopted solution consists on building these networks in the subsoil (Cui & Nelson, 2019). However, in large cities the underground space is also congested by the existence of different types of infrastructures (Bobylev, 2016), which often leads to the construction of new tunnels in close proximity to existing ones, or to the construction of twin tunnels close to each other. In this case, one of the most important aspects in the design stage is to assess the existence of interaction between tunnels and how it might affect the ground deformations and the forces on its linings.

Evidences of twin tunnel interaction have been reported by many case studies (e.g. Bartlett & Bubbers, 1970; Cording & Hansmire, 1975; Nyren, 1998; Afifipour et al., 2011; Ocak, 2014; Fargnoli et al., 2015; Elwood & Martin, 2016; Wan et al., 2017), which concluded, based on the monitoring data, that the second tunnel (2T) excavation induced higher movements than those associated with the construction of the existing/first tunnel (1T). Mair & Taylor (1997) justified this behaviour with the disturbed ground conditions where the 2T is excavated and identified the pillar width between tunnels as a key parameter in the interaction. Numerical (e. g. Addenbrooke & Potts, 2001; Ng et al., 2004; Do et al., 2015), centrifuge (Wu & Lee, 2003; Divall & Goodey, 2015) and small-scale (Kim et al., 1998; Chapman et al., 2007) models reached similar conclusions and observed that the interaction between tunnels was particularly relevant for a ratio of the pillar width (L) to the diameter of tunnel (D) smaller than one ($L / D < 1.0$). A compilation and a thorough review of the studies published in the literature about the influence of twin tunnelling on the ground deformations was presented by Do et al. (2014b) and, more recently, by Islam & Iskander (2021). However, as stated by Do et al. (2014b), most of those studies are focused on the deformations measured at ground surface, while the evaluation of the lining forces induced by the 2T excavation on both tunnels is often disregarded or seen as a minor aspect. Following a strategy similar to the previous studies the aim of this paper is to contribute to a better knowledge of these aspects by performing a thorough numerical analysis. The influence of crucial parameters, such as the stiffness of the lining and the initial stress conditions, on the lining forces of both tunnels were also assessed. For that purpose, a series of 2D numerical analyses of the sequential

#Corresponding author. E-mail address: amgpedro@dec.uc.pt
[1]Universidade de Coimbra, Instituto para a Sustentabilidade e Inovação em Estruturas de Engenharia, Departamento de Engenharia Civil, Coimbra, Portugal.
[2]Universidade de Coimbra, Departamento de Engenharia Civil, Coimbra, Portugal.

Submitted on November 15, 2021; Final Acceptance on June 3, 2022; Discussion open until November 30, 2022.
https://doi.org/10.28927/SR.2022.077221

excavation of side-by-side twin tunnels was carried out using the in-house finite element program, UCGeoCode, developed at the Department of Civil Engineering of the University of Coimbra (Sousa, 1998; Grazina, 2009).

2. Background on lining forces induced by twin tunnelling

Table 1 summarizes the main results published in the literature that refer the impact of side-by-side twin tunnelling in the stresses and forces acting on the lining. From the thirteen research studies compiled eleven are based on numerical analysis (2D and 3D) and only two (Adachi et al., 1993; Kim et al., 1998) used 1g small-scale models, highlighting the lack and need of real monitoring data to support their conclusions. However, it is worth mentioning the recent study conducted by Cheng et al. (2020) which, in spite of analysing a piggyback (one tunnel above the other) rather than a side-by-side configuration, compared the numerical results against field measurements with the results showing a good agreement in terms of the hoop forces predicted in the 1T.

The initial research on the topic was performed by Ghaboussi & Ranken (1977) and Soliman et al. (1993) and confirmed its relevance with the results showing a significant increase of the forces in the lining of the 1T after the excavation of the 2T. The lining of the 2T also presented higher forces when compared with those determined in a greenfield scenario, i.e., without the presence of the 1T, although of smaller magnitude. However, in those studies a linear elastic model was adopted for the soil, which is an unrealistic assumption. In the following studies, more realistic constitutive models were adopted for the soil, with the majority considering the elastic-perfectly plastic Mohr-Coulomb failure criterion or equivalent. These studies mainly assessed the influence of the distance between tunnels (pillar width) and, recurring to 3D analysis, the lagged distance between the two excavation faces. In line with the elastic results, and despite the differences among the analysis, all studies concluded that significant interaction occurred for $L / D < 1.0$, with a considerable increase of the lining forces in the 1T while a moderate increase was observed on the 2T. In all cases the maximum variations of the lining forces were observed at the pillar springline (i.e. the springline closest to the other tunnel). Most studies also observed that for L / D > 2.0 there is no noticeable variation on the lining forces of both tunnels, suggesting that this ratio corresponds to the maximum interaction distance between tunnels. Kim et al. (1998) results showed that the stiffness of the lining has a reduced influence on the bending moments of the 1T, but these results were obtained employing very flexible supports, which are not ideal to characterise the lining behaviour (Peck et al., 1972). The effect of the initial stress conditions was also not thoroughly analysed with most studies using a constant depth of the tunnel and a coefficient of earth pressure at rest (K_0) value of about 0.5. The exceptions are the elastic study of Ghaboussi & Ranken (1977) where a moderately increase of the lining forces was observed for greater depths and the research performed by Adachi et al. (1993) which found that the interaction between tunnels appears to increase with the increase of the overburden. Despite using significantly higher and even non-constant K_0 values, Ng et al. (2004) and Liu et al. (2008) obtained results similar to those presented by the other studies and did not investigate the influence of using different initial stress conditions.

All these studies represent a valid effort towards understanding how the lining of the tunnels are affected by twin tunnelling, since it is extremely unlikely to be able to investigate based on real cases due to the rigid geometry configurations that are usually imposed and due to the absence of monitoring data available. As a result, the most common option to analyse the problem is by conducting vast numerical studies where the influence of the different parameters is analysed through parametric studies.

3. Methodology employed

Figure 1 shows the layout of the geometry adopted in all 2D plane strain analyses. For the reference analyses a depth of the tunnel axis (H) of 19 m (cover of 16 m) was adopted, while the circular tunnels had a diameter

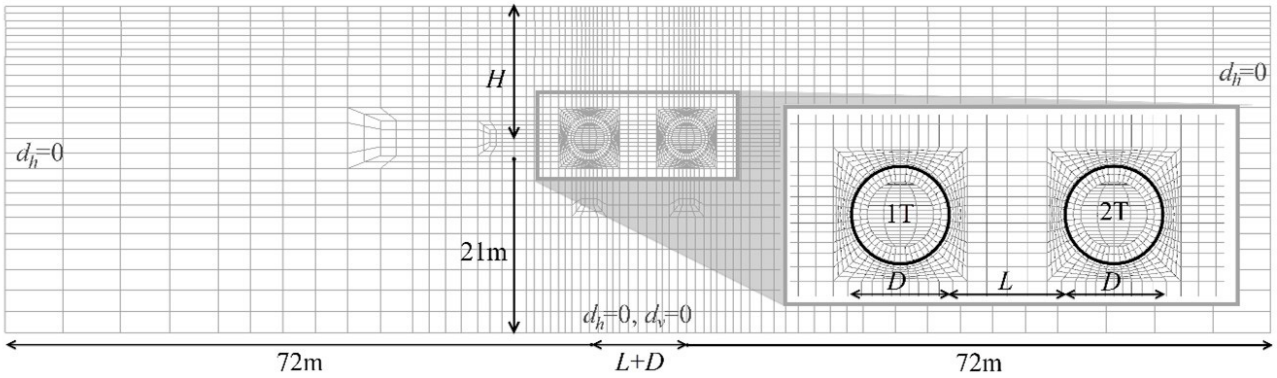

Figure 1. Layout of the geometry and finite element mesh for the model with $L / D = 1.0$.

Table 1. Summary of the relevant studies about pressures and lining forces induced by twin tunnelling.

References	Geotechnical soil model	Tunnel geometry	Method of analysis	Main results about pressures and lining forces
Ghaboussi & Ranken (1977)	Linear elastic $K_0 = 0.5$	D = (?) m H / D = 1.5; 5.5 L / D = 0.25 to 1.0	Numerical 2D Excavation in full section	Increase of forces in the lining in the zone around the pillar springline in both tunnels; Interaction more relevant for deep tunnels; Suggest no interaction for $L / D > 2.0$
Soliman et al. (1993)	Linear elastic Stiffness of the ground varied $K_0 = 0.5$	D = 10 m H / D = 3.5 L / D = 0.25; 0.5	Numerical 2D / 3D Excavation in full section	Increase of forces in the lining of both tunnels; Bending moments are more affected by the 2T excavation but no trend was observed with the increase of stiffness of the ground
Adachi et al. (1993)	Sand c' = 0 kPa; ϕ' = 30° $K_0 \approx 0.7$	D = 130 mm H / D = 1.0 to 4.5 L / D = 0.5 to 2.0	Small scale 1g model Excavation in full section by reducing the diameter	Interaction between tunnels increases with the increase of the overburden. Interaction still occurs for $L / D = 2.0$
Kim et al. (1998)	Speswhite kaolin clay $S_u \approx 20$ kPa $K_0 \approx 0.5$	D = 70 mm H / D = 3.2 L / D = 0.4; 1.0	Small scale 1g model Simulation of an EPB-TBM	Interaction between tunnels was observed with an increase of the bending moments on the 1T at the pillar springline
Ng et al. (2004)	Drucker-Prager (equivalent Mohr-Coulomb: c' = 5 kPa; ϕ' = 22°) $K_0 = 1.5$	$D \approx 8.6$ m (Oval) H / D = 2.3 L / D = 1.0	Numerical 3D NATM modelling with 2 side-drifts and variable lagged distance	Increase of the lining forces (bending and hoop) of the 1T with the increase of the lagged distance; The lining forces on both tunnels are minimum for a zero lagged distance
Hage Chehade & Shahrour (2008)	Mohr–Coulomb (c' = 3 kPa; ϕ' = 33°) $K_0 = 0.5$	D = (?) m H / D = 2.5 L / D =1.0 to 4.0	Numerical 2D (β = 0.5) Excavation in full section	No interaction was detected on the hoop forces while a residual increase was observed on the bending moments for $L / D < 2.0$
Liu et al. (2008)	Mohr–Coulomb (c' = 500 kPa; ϕ' = 38°) K_0 varies with depth and direction	$D \approx 10$ m (Oval) H / D = 1.5; 3.0 L / D = 1.0; 2.0	Numerical 3D NATM modelling with excavation in full section	Stresses in the 1T lining increase after the 2T excavation; Interaction increases with the decrease of the pillar width
Hossaini et al. (2012) (Section 1)	Mohr–Coulomb (c' = 0 kPa; ϕ' = 35°) $K_0 = 0.43$	D = 6.9 m H / D = 1.9 L / D = 0.5 to 1.5	Numerical 3D Simulation of an EPB-TBM	Increase of forces (bending and hoop) in the lining of 1T after the 2T excavation; Minimum interaction for $L / D > 1.5$
Do et al. (2014a)	Mohr–Coulomb (c' = 0 kPa; ϕ' = 37°) $K_0 = 0.5$	D = 94 m H / D = 2.1 L / D = 0.25 to 3	Numerical 2D (β = 0.3) Excavation in full section	Relevant increase of the hoop forces on both tunnels (mainly on 1T) while only a slight variation observed on the bending moments; Interaction is relevant for $L / D < 1.0$ and more relevant if in a jointed lining; Negligible interaction for $L / D > 2.0$
Do et al. (2015)	CY soil model (c' = 0 kPa; ϕ' = 37°) $K_0 = 0.5$	D = 9.4 m H / D = 2.1 L / D = 0.25 to 2	Numerical 3D Simulation of an EPB-TBM considering a lagged distance of 10D	Relevant increase of the lining forces (bending and hoop) on the 1T; Slight decrease of the lining forces (bending and hoop) on the 2T; Negligible interaction for $L / D > 1.0$
Do et al. (2016)	CY soil model (c' = 0 kPa; ϕ' = 37°) $K_0 = 0.5$	D = 9.4 m H / D = 2.1 L / D = 0.25	Numerical 3D Simulation of an EPB-TBM considering variable lagged distance	Increase of the hoop forces of both tunnels with the lagged distance, while the opposite occurs for the bending moments; The lining forces on both tunnels are minimum for a zero lagged distance

Table 1. Continued...

References	Geotechnical soil model	Tunnel geometry	Method of analysis	Main results about pressures and lining forces
Shivaei et al. (2020)	Modified Cam-Clay (M = 1.14; κ = 0.011; λ = 0.048) K_0 = 0.55	D = 6.9 m H / D = 2.75 L / D = 1.2	Numerical 3D (coupled-consolidation) Simulation of an EPB-TBM Consolidation of the soil after the complete excavation of each tunnel	Increase of the lining permeability from impermeable to fully permeable originates an increase of the lining forces (bending and hoop) on both tunnels, which is more relevant on the 1T on the pillar side;
Cheng et al. (2020)	Mohr–Coulomb (c' = 5 kPa; ϕ' = 33.3°) K_0 = 0.7	D = 6.1 m H / D = 3.5 (1T) L / D = 0.4 (2T above 1T)	Numerical 2D (β = 0.1) Excavation in full section Piggyback configuration	Good agreement of the hoop forces between the numerical predictions and the field measurement

(D) of 6 m and were spaced of a distance (L) which varied between a minimum value of 1.5 m and a maximum value of 24 m, corresponding to extreme L / D ratios of 0.25 and 4.0, respectively. A continuous lining with 0.3 m thick was considered in both tunnels. Different values for the depth and diameter of the tunnels and for the thickness of the lining were adopted to assess their influence on the lining forces.

The finite element meshes employed in the analyses were different according with the geometries adopted. In all cases the tunnels were centred in the mesh and both the soil and the lining were discretized with quadrilateral solid elements, each with eight nodal points and four Gauss points for displacement and stress evaluation, respectively. To ensure the complete stabilisation of both stress and strain fields induced by the excavations a lateral distance of 72 m was adopted, measured from the centrelines of the nearest tunnel to the model external right/left border, while the bottom boundary was placed at 21 m below the invert of the tunnels (Figure 1). In terms of boundary conditions, no horizontal displacements (d_h = 0) were allowed along the lateral boundaries of the mesh, while at the bottom the displacements were constrained in both directions (d_h = 0, d_v = 0). No restriction of displacements was imposed at the top of the model, coincident with the ground surface. Drained conditions were assumed in all analyses and consequently no hydraulic boundaries were prescribed. In order to improve the accuracy of the results a high discretization and density of elements around the tunnels and on the linings was adopted (Figure 1).

In line with the most recent studies (Table 1) a perfectly plastic non-associated Mohr-Coulomb yield criterion was adopted for describing the soil strength. For the stiffness a modified version of the power law proposed by Janbu (1967), where the deformability modulus varies throughout the analysis with the minimum principal effective stress (Equation 1), was employed.

$$E_s = E_0 + A \times p_{ref} \times \left(\frac{\sigma'_3}{p_{ref}} \right)^n \quad (1)$$

The values adopted for the soil parameters are presented in Table 2 and were established having as reference the values employed by the previous studies in order to facilitate the comparison of results. As for the lining a linear elastic behaviour, characterised by a Poisson's ratio (ν_l) of 0.2 and a Young's modulus (E_l) of 30 GPa, was adopted to simulate the pre-cast concrete segments.

To establish the initial geostatic stresses in the model the vertical stresses were calculated assuming a unit weight of 20 kN/m^3 while the horizontal stresses were determined by considering a constant K_0 of 0.6.

Modelling the excavation of a tunnel in 2D requires simplifications and assumptions in order to account for the 3D effects of the excavation of the tunnel. From the diverse approaches available in the literature (Möller, 2006) the stress reduction method is the most common and was adopted in the present study. This method simulates the excavation in two stages. In the first, the elements inside the tunnel are removed and the initial ground pressure (p_0) acting on the tunnel contour, is reduced of (1 - β) × p_0. In the second stage the lining is installed and the remaining load, β × p_0, applied so that a final equilibrium state is achieved. As demonstrated by Möller & Vermeer (2006) the selection of an appropriate load reduction factor (β) is one of the difficulties of the method. Their study concluded that the adoption of one single β-value is not suitable for reproducing both the lining forces and the displacements observed in the 3D calculations and suggested using β-values between 0.3 and 0.4 to properly match the displacements, while for the lining forces higher values, in the range of 0.5 to 0.7, are recommended. Given the purpose of this investigation a value of 0.6, in line with the suggestion of Möller & Vermeer (2006), was adopted in all analyses. For modelling the sequential excavation of

both tunnels this procedure was adopted separately for each tunnel, first for the left tunnel (1T) and then for the right tunnel (2T), resulting in a total of four stages.

4. Influence of the pillar width

The influence of the pillar width on the hoop force and bending moment of both tunnels for the final stage (i.e. after the 2T excavation) is illustrated in the radial diagrams presented in Figure 2, for six L / D ratios, varying from 0.25 to 4.0. For ease of comparison the values obtained in greenfield conditions, i.e., immediately after the 1T excavation (stage 2), are also superimposed on the figures. As expected and in agreement with the results of Möller (2006), the hoop forces obtained in greenfield conditions are always compressive and symmetrical in relation to the tunnel centreline, exhibiting higher values at the springline, of around 654 kN/m, in correspondence with the squat of the lining caused by the K_0 being smaller than one. At the invert the hoop forces are slightly higher (≈ 445 kN/m) than those determined at the crown (≈ 383 kN/m) as a result of the higher geostatic pressure. The bending moments in greenfield conditions exhibit a maximum negative value at the springline (≈ - 64 kNm/m) and a slightly smaller positive value at the invert and crown (≈ 61 kNm/m). The inversion of sign of the bending moment is also associated with the deformation shape of the lining and occurs around the shoulder and knee of the lining, being positive (sagging) within these locations and negative (hogging) in the other parts of the lining.

Figure 2 shows that for $L / D > 2.0$ the final lining forces on both tunnels are similar to those determined for greenfield conditions, implying that the 2T excavation had a minimal impact on the lining forces and consequently the interaction effects appear to be minimal. For smaller L / D the lining forces surpass those determined for greenfield conditions and increase with the decrease of the pillar width, reaching a maximum for $L / D = 0.25$. This behaviour is in agreement with the results of Do et al. (2014a, 2016) and confirms that the interaction between tunnels leads to an increase of the lining forces in both of them. The increase in both hoop forces and bending moments is more relevant in the 1T with the highest variations observed on the side of the 2T, with a maximum at the pillar springline, as noted by Kim et al. (1998). In the 2T the lining forces variations are smaller but are also primarily concentrated around the pillar springline (i.e,. springline closest to the 1T in this case).

To facilitate the comprehension of the results the maximum absolute values of the lining forces (F_{Final}) are normalised by the respective greenfield values ($F_{Greenfield}$) and replotted in Figure 3 against the L / D ratio. The plot confirms that maximum interaction occurs for tunnels closely spaced and tend to decrease with the increase of the pillar width, being residual for $L / D = 2.0$ and negligible for $L / D > 3.0$. The trend observed for both lining forces is similar in each tunnel with the bending moments presenting a slightly more pronounced decay. For the 1T (solid lines) a maximum increase of about 30% and 27% is observed on the hoop force and bending moment, respectively, for a $L / D = 0.25$. However, for the same L / D, the increase in the 2T lining forces (dashed lines) is considerably smaller and does not surpass 12%, with the bending moment being slightly higher in this case.

5. Stiffness of the lining

The forces acting on the lining are influenced by the relative stiffness between the soil and the lining, which can be evaluated by recurring to two dimensionless coefficients,

Table 2. Soil parameters adopted in the reference analysis.

γ (kN/m³)	ϕ' (°)	c' (kPa)	ψ (°)	E_0 (kPa)	A	n	p_{ref} (kPa)	ν_s	K_0
20	35	5	5	5000	400	0.5	100	0,3	0.6

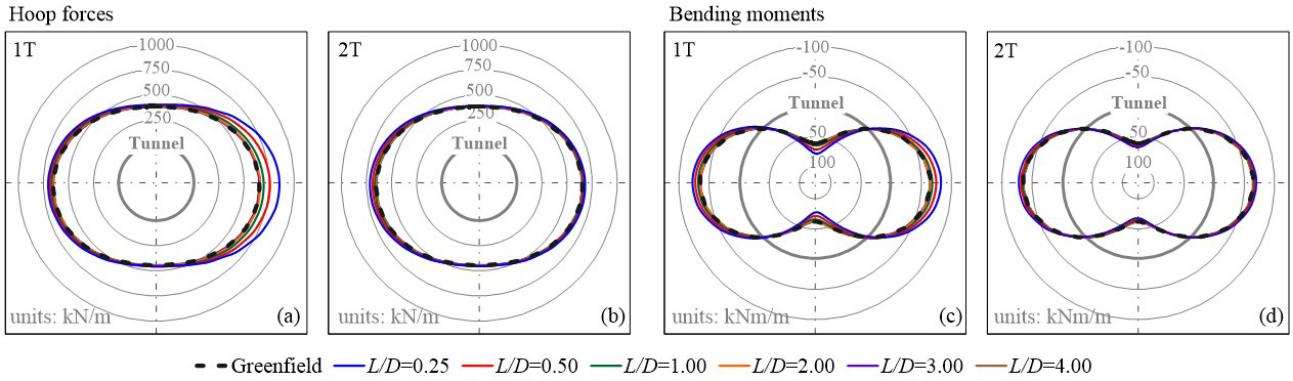

Figure 2. Radial diagrams of the hoop forces and bending moments acting on the lining for the reference analyses on both tunnels.

the compressibility (c) and the flexibility (f) ratios (Peck et al., 1972), as expressed in the following equations:

$$c=\frac{E_s \times R \times \left(1-\nu_l^2\right)}{E_l \times t\left(1+\nu_s\right)\left(1-2\nu_s\right)} \quad (2)$$

$$f=\frac{E_s \times R^3 \times \left(1-\nu_l^2\right)}{6 \times E_l \times I \times \left(1+\nu_s\right)} \quad (3)$$

where E_l and ν_l are the Young's modulus and Poisson's ratio of the lining and E_s and ν_s are the equivalent values of the soil determined for the depth of the tunnel axis. R is the radius of the tunnel and t and I refer to the thickness and moment of inertia of the lining cross-section. The compressibility ratio (c) is a measure of the extensional stiffness of the soil relative to that of the lining under a uniform external pressure, while the flexibility ratio (f) is associated with the relative flexural stiffness under a state of pure shear. The results of Peck et al. (1972) show that the flexibility ratio is particularly relevant when analysing the lining behaviour. As confirmed by Kim et al. (1998) tests, for flexibility ratios higher than 10 the lining can be considered flexible and no substantial variations on the bending moments values should be expected.

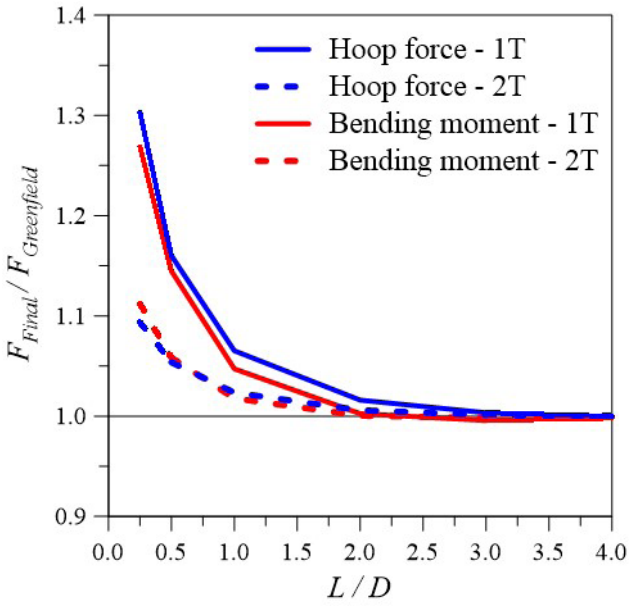

Figure 3. Influence of the pillar width on the lining forces.

In order to clarify the influence of the stiffness of the lining three sets of analyses were carried out. In these the geometrical characteristics of the tunnels and linings were chosen so that preferably stiffer, though realistic, linings were obtained, while the stiffness properties of both soil and lining were kept equal to the reference values to better isolate and assess the effects of the variable parameters. In Set A, the thickness (t) of the lining was varied from 0.15 to 0.6 m, while keeping the diameter of the tunnel constant with 6 m. In set B, diameters of the tunnel of 4, 6 and 8 m were adopted under a constant aspect ratio, D / t, equal to 20. In the third set (Set C) two additional analyses were performed to explore extreme scenarios, one with a tunnel diameter of 4 m and D / t = 10 representing a very stiff lining, and the other with a diameter of 8 m and D / t = 40 corresponding to a flexible lining. The geometrical characteristics of the tunnels and linings employed in the three sets of analyses are presented in Table 3.

The results of the lining forces are presented in Figure 4 for the three sets of analyses. In the radial diagrams the hoop forces and bending moments obtained in greenfield conditions are represented, while in the other plots the final normalized maximum values are plotted against the L / D ratio for both tunnels. The results of Set A are displayed on the left side (corresponding to plots (a), (b), (e) and (f)) while Set B and C are depicted on the right (corresponding to plots (c), (d), (g) and (h)). Looking at the effect on the hoop forces, and in spite of the significant variation of the thickness of the lining considered in the analyses, the results obtained in greenfield conditions are similar with only a maximum variation of about 8% observed at the tunnel springlines between the two extreme cases analysed, 15 and 60 cm thick (Figure 4a). These results can be related with the compressibility ratio, which is small and of the same magnitude in all analyses, indicating that the lining is considerably stiffer than the soil. Furthermore, the interaction effects observed in the hoop force after the

Table 3. Geometrical characteristics of the tunnels and linings employed in the analyses.

Set	A					B			C	
Designation	t=15cm	t=20cm	***t*=30cm**	t=40cm	t=60cm	***D*4-*D*/ *t*=20**	*D*6-*D*/ t=20	*D*8-*D*/ t=20	*D*4-*D*/ t=10	*D*8-*D*/ t=40
D (m)	6	6	6	6	6	4	6	8	4	8
C (m)	16	16	16	16	16	16	16	16	16	16
H (m)	19	19	19	19	19	18	19	20	18	20
t (cm)	15	20	30	40	60	20	30	40	40	20
D / t	40	30	20	15	10	20	20	20	10	40
c	3.8×10^{-2}	2.8×10^{-2}	1.9×10^{-2}	1.4×10^{-2}	9.4×10^{-3}	1.8×10^{-2}	$1.9\times^{-2}$	1.9×10^{-2}	9.2×10^{-3}	3.8×10^{-2}
f	12.0	5.1	1.5	0.6	0.2	1.5	1.5	1.5	0.2	12.3

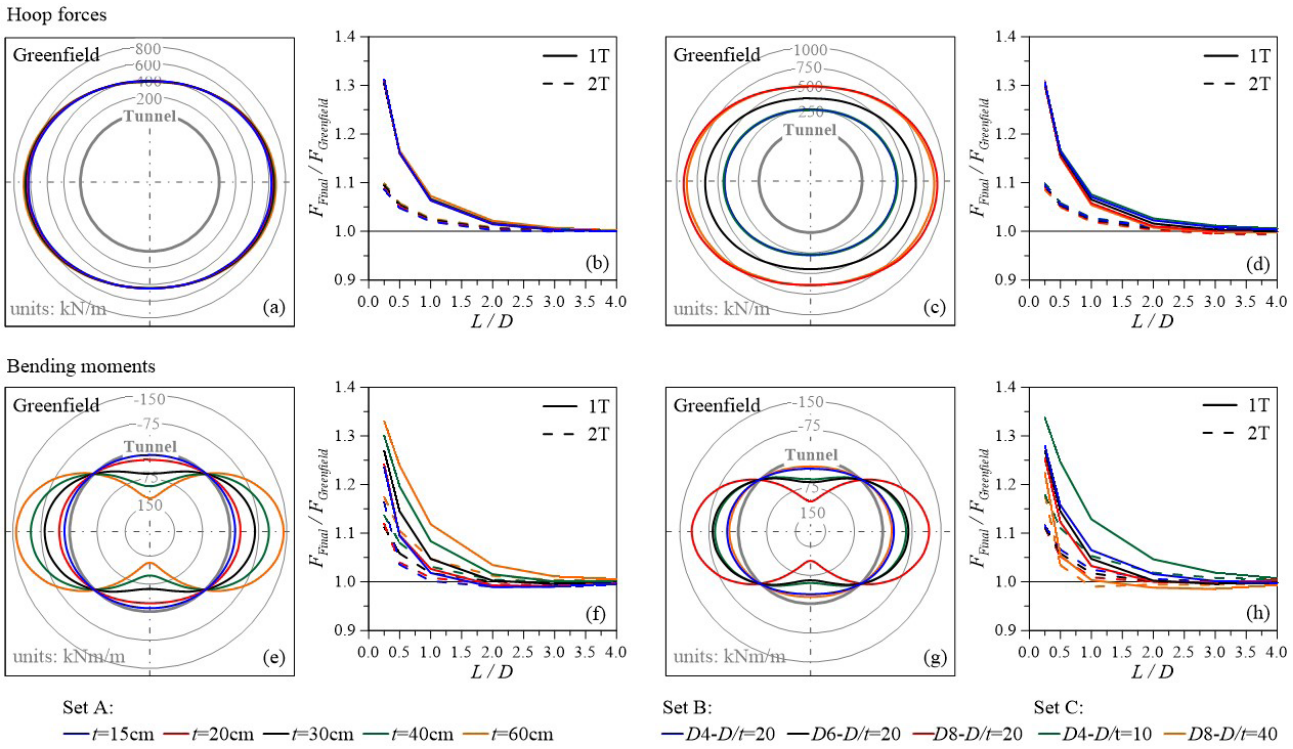

Figure 4. Influence of the thickness and of the tunnel lining aspect ratio on the lining forces.

2T excavation are also almost independent of the thickness of the lining with a similar behaviour observed in all cases (Figure 4b). Naturally, and as mentioned in the previous section, the interaction affects mainly the 1T, although the increase of forces cannot be neglected for $L / D < 2.0$ in both tunnels. Figure 4c shows that the diameter of the tunnel under a constant aspect ratio only scales the magnitude of the hoop forces, while its overall behaviour remains equal. As expected, a higher diameter of the tunnel corresponds to higher hoop forces since the excavated soil mass increases considerably. In similarity with the previous results and in agreement with the compressibility ratio interpretation it is also verified that the influence of the thickness on the hoop force is also minimal when the diameter of the tunnel is varied. The results of the tunnel interaction (Figure 4d) show that despite all analyses presenting a similar value for $L / D = 0.25$ a slightly higher decay, predominantly observed in the 1T, is visible with the increase of the tunnel diameter. Nevertheless, the overall behaviour is very similar in all analyses and suggests that the hoop forces are not significantly affected by changing the geometrical characteristics of the lining, particularly if linings with small compressibility ratios are considered.

In contrast with the observed in the hoop forces, the bending moments values are influenced by the thickness of the lining in greenfield conditions and tend to increase considerably for thicker linings (Figure 4e). In agreement with Peck et al. (1972) results, as the thickness reduces the lining becomes flexible and the bending moments became smaller and uniform. The thickness of the lining also influences the bending moment distribution when the 2T is excavated. Figure 4f shows that for greater thicknesses the interaction increases in magnitude and extends to a further distance, reaching $L / D = 3.0$ for a thickness of 60 cm. The increase in magnitude is observed in both tunnels, although continues greater in the 1T. As shown in Figure 4g, the diameter of the tunnel under constant aspect ratio (Set B) also affects the bending moments in greenfield conditions. As the diameter of the tunnel increases the bending moments also increase, though the overall behaviour remains similar in all cases, with the maximum absolute values observed at the springlines. The extreme cases analysed in Set C confirmed the influence of the thickness on the bending moments, with higher values obtained in the stiffer lining ($D4$-D/t=10) and smaller in the flexible lining ($D8$-D/t=40) in comparison with the results of the analyses with the same diameter and $D / t = 20$. Also in this case the interaction effects observed in the bending moments depend on the diameter of the tunnel under constant aspect ratio as it can be seen by the results of Set B (Figure 4f). For $D / t = 20$ the interaction between tunnels tends to decrease slightly when larger diameters are considered, though it is still relevant in both tunnels for $L / D < 2.0$. The two extreme cases analysed in Set C clearly show that the interaction effects tend to increase in magnitude and extension (negligible only for $L / D > 3.0$) when stiffer

linings are considered and is minor and only relevant for $L / D < 1.0$ when flexible linings are employed.

6. Initial stress conditions

The initial stress conditions are a fundamental aspect in tunnelling since their orientation and value directly influences the distribution and magnitude of the forces acting on the lining. In order to further explore this aspect two additional sets of analyses were performed. In Set D, the effect of the overburden was analysed by varying the cover (C) of the tunnel from 8 to 32 m, while keeping a constant K_0 value equal to 0.6. In the second set (Set E) the cover was kept constant as 16 m while the K_0 value was varied from 0.4 to 1.2 in order to evaluate the influence of the lateral stresses. All other parameters were unchanged and kept equal to those employed in the reference analyses.

The results of the lining forces are presented in Figure 5 for the two sets of analyses. In the radial diagrams the hoop forces and bending moments obtained in greenfield conditions are represented, while in the other plots the final normalized maximum values are plotted against the L/D ratio for both tunnels. The results of Set D are displayed on the left side (corresponding to plots (a), (b), (e) and (f)) while Set E is depicted on the right (corresponding to plots (c), (d), (g) and (h)). Figure 5a shows that the increase in overburden translates in an almost proportional increase of the hoop forces in greenfield conditions, with the minimum values observed for a cover of 8 m and the maximum for 32 m. The overburden of the tunnels marginally influences the interaction effects on the hoop forces, which continue to be significant for $L / D < 1.0$ and negligible for $L / D > 3.0$ (Figure 5b). The exception is the analysis with the minimum cover of 8 m, where a higher decay of the interaction is visible, suggesting that for shallower tunnels the interaction only occurs when the tunnels are closely spaced ($L / D < 2.0$). This result is in agreement with Adachi et al. (1993) observations and is justified by the impossibility of the typical yielding zones observed in shallower tunnels fully develop and transfer load to the other tunnel due to the small cover.

The influence of the K_0 on the hoop forces for greenfield conditions is plotted in Figure 5c. With the increase of the K_0 the behaviour of the lining is modified and the hoop forces at the crown and invert tend to increase due to the higher lateral stresses, while the forces at the springline remain approximately constant since the overburden is equal in all analyses. For a $K_0 = 1.0$ an almost uniform hoop force is observed throughout the entire lining, with just a slight increase in depth due to the higher geostatic stresses, while for a $K_0 = 1.2$ the maximum hoop forces became located at the invert and crown. The analysis of the interaction plot (Figure 5d) shows that the maximum hoop forces in the lining present a similar behaviour for K_0 smaller than 1.0, with the typical increase of forces on both tunnels, higher in the 1T, with the decrease of the pillar width. However, for a $K_0 \geq 1.0$ a considerable modification occurs with the

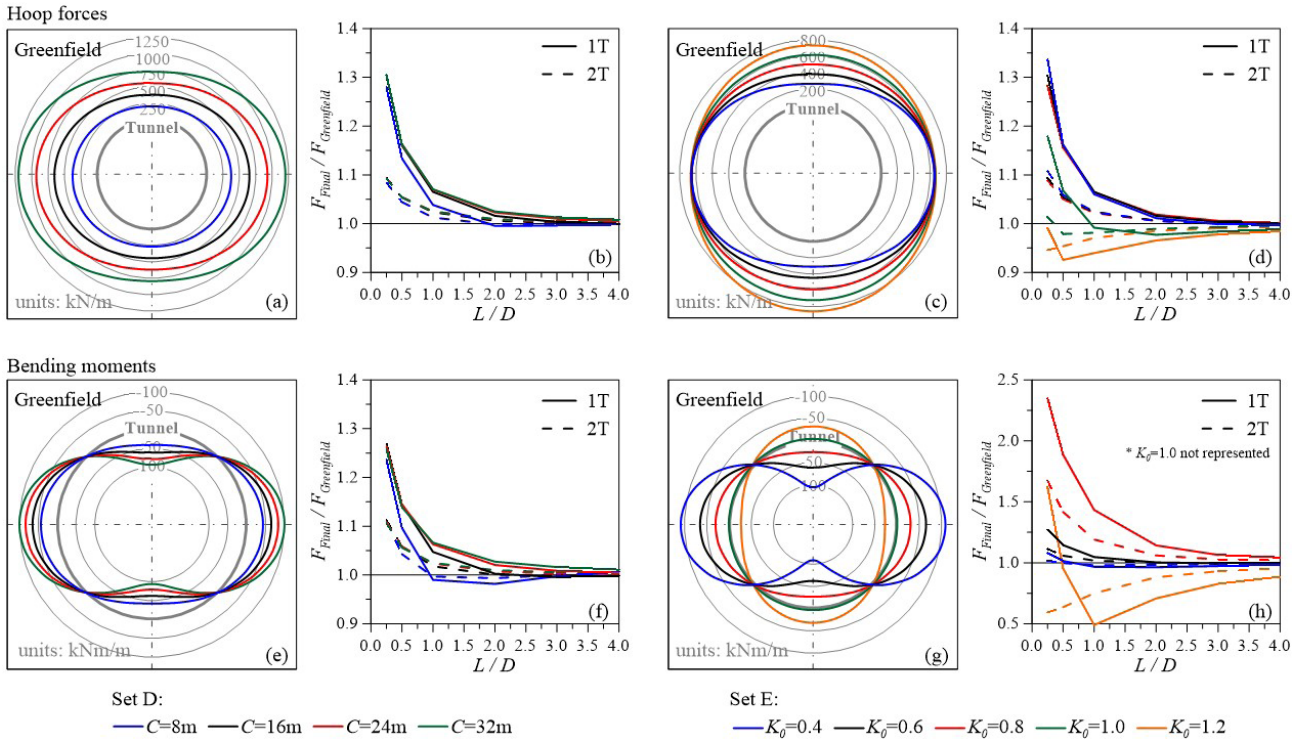

Figure 5. Influence of the cover and of the K_0 on the lining forces.

final maximum forces becoming inclusively smaller than those determined in greenfield conditions, for almost all L / D ratios when $K_0 = 1.0$ and for all pillar widths when $K_0 = 1.2$. Naturally, with the increase of the pillar width all analyses tend to converge towards zero interaction. In order to understand the behaviour observed when $K_0 \geq 1.0$ the distribution of hoop forces acting on the lining of both tunnels for the final stage are plotted in Figure 6 for the most relevant pillar widths ($L / D = 0.25$, 0.5, 1.0 and 2.0). From the plot it is possible to verify that with the 2T excavation the hoop forces in both tunnels tend to increase at the pillar springline and to decrease at the crown and invert with the decrease of the pillar width. Consequently, and in contrast with the previous analyses where the maximum hoop forces always occurred at the pillar springline, when $K_0 \geq 1.0$ the maximum values in the greenfield and final stages do not occur at the same location. As a result, an overall relative reduction in the final hoop forces can occur in the lining as shown in Figure 5h, since only the maximum values are considered in the plot, regardless of their location at the lining. However, it should be noted that in some parts of the lining, namely at the pillar springline, a substantial increase of forces should be expected due to the 2T excavation.

The influence of the overburden on the bending moments is also presented in Figure 5. The greenfield results show that the increase of the cover translates in moderately higher bending moments as a result of the higher stresses, though the overall behaviour of the lining remains unchanged (Figure 5e). The interaction effects observed in the bending moments after the 2T excavation depend on the overburden of the tunnel and present a similar trend to that observed on the hoop forces but with a slightly more pronounced decay (Figure 5f). For the analysis with a cover of 8 m the influence of the presence of the 1T is just relevant for $L / D < 1.0$, confirming that shallower tunnels only interact if closely spaced.

Figure 5g shows that the K_0 value influences the bending moments distribution in greenfield conditions. For $K_0 < 1.0$ the lining squats and consequently positive bending moments are obtained at crown and invert, while negative values are determined at the springlines. However, when $K_0 > 1.0$ the lining deformation shifts from squatting to egging, with the consequent inversion of signal of the bending moments. In the particular case where $K_0 = 1.0$ the bending moments are nearly zero due to the almost symmetrical loading. The K_0 value also affects significantly the bending moments induced by the 2T excavation as it can be seen in Figure 5h. With the increase of the K_0 value up to 1.0 a significant increase of the bending moments is observed on both tunnels. For a $K_0 = 0.8$ an increase of the bending moments of nearly 230% and 170% is observed in the 1T and 2T, respectively, and even higher variations are obtained for a $K_0 = 1.0$ (not represented in the figure). However, these increases are exponentiated by the almost zero values determined in greenfield conditions and correspond to final bending moments of moderate magnitude as it can be seen in Figure 7. In contrast, for a $K_0 = 0.4$ almost no interaction between tunnels is observed with only a slight increase of forces obtained for $L / D = 0.25$. The different behaviour observed for $K_0 = 1.2$ in both tunnels, is again justified by

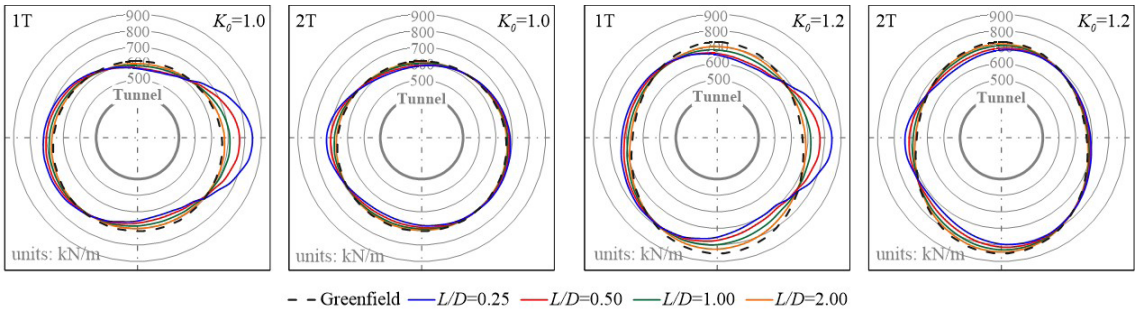

Figure 6. Radial diagrams of the hoop force acting on the lining for the $K_0 = 1.0$ and $K_0 = 1.2$ analyses.

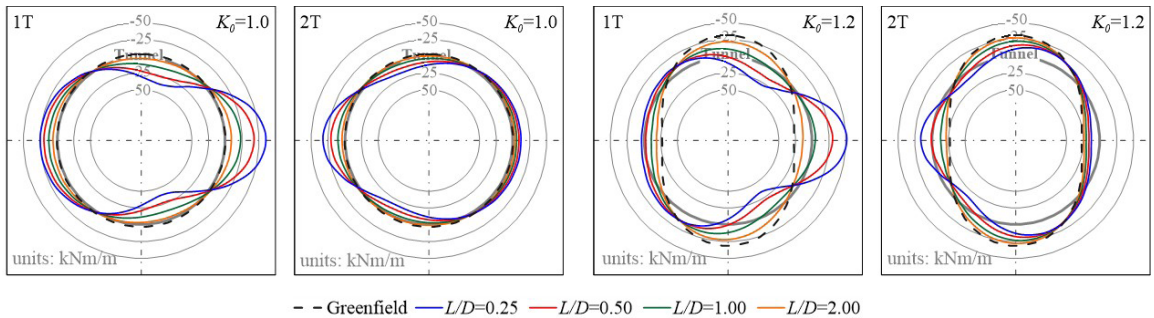

Figure 7. Radial diagrams of the bending moment acting on the lining for the $K_0 = 1.0$ and $K_0 = 1.2$ analyses.

the different location in the lining of the maximum absolute values of bending moment as can be seen in Figure 7. Also in this case, the excavation of the 2T originates an increase of bending moments at the pillar springline and a decrease at the invert and crown, inverting the position where the maximum values were observed in greenfield conditions.

7. Conclusions

It is well recognised that the excavation of a tunnel in close proximity to an existing one induces in the soil higher deformations due to the interaction effects between the tunnels. Furthermore, the second excavation also has an impact on the lining forces of both tunnels which is necessary to assess in order to design a lining capable to withstand the variations of forces induced by the excavation. In order to assess the influence of the flexibility and compressibility of the tunnel and of the initial stress conditions on the lining forces of both tunnels a series of 2D numerical analyses of side-by-side twin tunnels is carried out in this paper for a vast range of pillar widths and tunnel geometries. Based on the achieved results the following conclusions can be drawn:

- The results confirm that the 2T excavation induces higher hoop forces and bending moments on the linings of both tunnels, with the interaction being significant for $L / D < 1.0$, residual for $L / D = 2.0$ and negligible for $L / D > 3.0$. The concentration of forces is essentially located at the pillar springline and is more relevant in the 1T, nearly 30%, although it cannot be neglected in the 2T where an increase of about 12% was still obtained for the same conditions;
- The thickness of the lining and the diameter of the tunnel marginally affected the increase of the hoop forces caused by tunnel interaction. In contrast, the bending moments are considerably influenced by those factors and an increase of the magnitude and of the extension of the interaction is observed when stiffer linings are employed;
- The increase of the overburden also does not influence the interaction between tunnels with similar curves being obtained for the lining forces. The exception was obtained for shallower tunnels suggesting that interaction only occurs if the tunnels are closely spaced due to the impossibility of the yielding zones above the tunnels to fully develop;
- The K_0 value influences considerably the lining behaviour and the interaction between tunnels. For $K_0 < 1.0$ the interaction is visible on the bending moments and increases with the increase of the K_0 value, while no noticeably differences in the interaction are observed in the hoop forces. For $K_0 \geq 1.0$ the lining deformation changes from squatting to egging in greenfield conditions and the maximum hoop forces and bending moments become located at the invert and crown. With the 2T excavation a reduction on both forces is observed at these locations while an increase is visible at the pillar springline. As a result, an overall relative reduction in the final forces occurs in the lining for all pillar widths if $K_0 = 1.2$ and for almost all L / D ratios if $K_0 = 1.0$.

The difficulties of finding real case studies where parameters such as the geometry and/or stiffness of the tunnel and/or the initial stress conditions vary significantly throughout the route makes this and the previous numerical studies valuable exercises in order to understand the behaviour of twin tunnels and to estimate the possible impact of a second excavation on an existing tunnel.

Declaration of interest

The authors have no conflicts of interest to declare. All co-authors have observed and affirmed the contents of the paper and there is no financial interest to report.

Authors' contributions

António Manuel Gonçalves Pedro: conceptualization, data curation, methodology, supervision, validation, writing – original draft. José Carlos Duarte Grazina: conceptualization, data curation, methodology, validation, writing – original draft. Jorge Nuno Veiga de Almeida e Sousa: conceptualization, methodology, validation, writing – review & editing.

List of symbols

c	Compressibility ratio
c'	Soil cohesion
d_h	Horizontal displacement at model boundaries
d_v	Vertical displacement at model boundaries
f	Flexibility ratio
n	Parameter of the Janbu's law
p_0	Initial ground pressure
p_{ref}	Reference stress (= 100 kPa)
t	Thickness of the lining
A	Parameter of the Janbu's law
C	Cover of the tunnel
D	Diameter of the tunnel
E_l	Young's modulus of the lining
E_s	Soil deformability modulus
E_0	Soil deformability modulus at ground surface
F_{Final}	Final maximum hoop force / bending moment value
$F_{Greenfield}$	Greenfield maximum hoop force / bending moment value
H	Depth of the tunnel axis
I	Inertia of the tunnel lining
K_0	At-rest earth pressure coefficient
L	Pillar width
M	Stress ratio (Cam-clay model)

R	Radius of the tunnel
S_u	Undrained strength
β	Load reduction factor
γ	Unit weight of the soil
$\phi\rangle$	Angle of shear resistance
κ	Slope of the swelling line (Cam-clay model)
λ	Slope of the normal compression (Cam-clay model)
ν_l	Poisson's ratio of the lining
ν_s	Poisson's ratio of the soil
$\sigma\rangle_3$	Minimum principal effective stress
ψ	Soil dilatancy angle

References

Adachi, T., Kimura, M., & Osada, H. (1993). Interaction between multi-tunnels under construction. In *Proceedings of the 11th Southeast Asian Geotechnical Conference* (pp. 51-60). Singapore.

Addenbrooke, T.I., & Potts, D. (2001). Twin tunnel interaction: surface and subsurface effects. *International Journal of Geomechanics*, 1(2), 249-271. http://dx.doi.org/10.1016/j.tust.2015.11.013.

Admiraal, H., & Cornaro, A. (2016). Why underground space should be included in urban planning policy – And how this will enhance an urban underground future. *Tunnelling and Underground Space Technology*, 55, 214-220. http://dx.doi.org/10.1016/j.tust.2015.11.013.

Afifipour, M., Sharifzadeh, M., Shahriar, K., & Jamshidi, H. (2011). Interaction of twin tunnels and shallow foundation at Zand underpass, Shiraz metro, Iran. *Tunnelling and Underground Space Technology*, 26(2), 356-363. http://dx.doi.org/10.1016/j.tust.2010.11.006.

Bartlett, J.V., & Bubbers, B.L. (1970). Surface movements caused by bored tunnelling. In *Proceedings Conference on Subway Construction* (pp. 513-539), Budapest.

Bobylev, N. (2016). Underground space as an urban indicator: measuring use of subsurface. *Tunnelling and Underground Space Technology*, 55, 40-51. http://dx.doi.org/10.1016/j.tust.2015.10.024.

Chapman, D.N., Ahn, S.K., & Hunt, D.V. (2007). Investigating ground movements caused by the construction of multiple tunnels in soft ground using laboratory model tests. *Canadian Geotechnical Journal*, 44(6), 631-643. http://dx.doi.org/10.1139/t07-018.

Cheng, W., Li, G., Ong, D.E.L., Chen, S., & Ni, J.C. (2020). Modelling liner forces response to very close-proximity tunnelling in soft alluvial deposits. *Tunnelling and Underground Space Technology*, 103, 103455. https://doi.org/https://doi.org/10.1016/j.tust.2020.103455

Cording, E.J., & Hansmire, W. (1975). Displacements around soft ground tunnels, general report: Session IV, Tunnels in soil. In *Proceedings of the 5th Pan American Conference on Soil Mechanics and Foundation Engineering* (pp. 571-633), Buenos Aires: Sociedad Argentina de Mecánica de Suelos e Ingenieria de Fundaciones.

Cui, J., & Nelson, J.D. (2019). Underground transport: an overview. *Tunnelling and Underground Space Technology*, 87, 122-126. http://dx.doi.org/10.1016/j.tust.2019.01.003.

Divall, S., & Goodey, R.J. (2015). Twin-tunnelling-induced ground movements in clay. *Geotechnical Engineering*, 168(3), 247-256. http://dx.doi.org/10.1680/geng.14.00054.

Do, N., Dias, D., & Oreste, P. (2015). 3D numerical investigation on the interaction between mechanized twin tunnels in soft ground. *Environmental Earth Sciences*, 73(5), 2101-2113. http://dx.doi.org/10.1007/s12665-014-3561-6.

Do, N., Dias, D., & Oreste, P. (2016). 3D numerical investigation of mechanized twin tunnels in soft ground–Influence of lagging distance between two tunnel faces. *Engineering Structures*, 109, 117-125. http://dx.doi.org/10.1016/j.engstruct.2015.11.053.

Do, N., Dias, D., Oreste, P., & Djeran-Maigre, I. (2014a). 2D numerical investigations of twin tunnel interaction. *Geomechanics and Engineering*, 6(3), 263-275. http://dx.doi.org/10.12989/gae.2014.6.3.263.

Do, N.-A., Dias, D., Oreste, P., & Djeran-Maigre, I. (2014b). Three-dimensional numerical simulation of a mechanized twin tunnels in soft ground. *Tunnelling and Underground Space Technology*, 42, 40-51. http://dx.doi.org/10.1016/j.tust.2014.02.001.

Elwood, D.E.Y., & Martin, C.D. (2016). Ground response of closely spaced twin tunnels constructed in heavily overconsolidated soils. *Tunnelling and Underground Space Technology*, 51(Suppl. C), 226-237. http://dx.doi.org/10.1016/j.tust.2015.10.037.

Fargnoli, V., Boldini, D., & Amorosi, A. (2015). Twin tunnel excavation in coarse grained soils: observations and numerical back-predictions under free field conditions and in presence of a surface structure. *Tunnelling and Underground Space Technology*, 49, 454-469. http://dx.doi.org/10.1016/j.tust.2015.06.003.

Ghaboussi, J., & Ranken, R.E. (1977). Interaction between two parallel tunnels. *International Journal for Numerical and Analytical Methods in Geomechanics*, 1(1), 75-103.

Grazina, J. (2009). *Dynamic modelling of elastoplastic massifs with viscous coupling. Application to flexible retaining walls under seismic loading*. [Doctoral thesis, University of Coimbra]. University of Coimbra's repository (in Portuguese). http://hdl.handle.net/10316/12076

Hage Chehade, F., & Shahrour, I. (2008). Numerical analysis of the interaction between twin-tunnels: influence of the relative position and construction procedure. *Tunnelling and Underground Space Technology*, 23(2), 210-214. http://dx.doi.org/10.1016/j.tust.2007.03.004.

Hossaini, S.M., Shaban, M., & Talebinejad, A. (2012). Relationship between twin tunnels distance and surface subsidence in soft ground of Tabriz Metro, Iran. In N. Aziz & B. Kininmonth (Eds.), *12th Coal Operators' Conference* (pp. 163-168). University of Wollongong.

Islam, M.S., & Iskander, M. (2021). Twin tunnelling induced ground settlements: a review. *Tunnelling and Underground*

Space Technology, 110, 103614. https://doi.org/https://doi.org/10.1016/j.tust.2020.103614

Janbu, N. (1967). *Settlement calculations based on the tangent modulus concept. Three guest lectures at Moscow State University.* Technical University of Norway.

Kim, S.H., Burd, H.J., & Milligan, G.W.E. (1998). Model testing of closely spaced tunnels in clay. *Geotechnique*, 48(3), 375-388. http://dx.doi.org/10.1680/geot.1998.48.3.375.

Liu, H.Y., Small, J.C., & Carter, J.P. (2008). Full 3D modelling for effects of tunnelling on existing support systems in the Sydney region. *Tunnelling and Underground Space Technology*, 23(4), 399-420. http://dx.doi.org/10.1016/j.tust.2007.06.009.

Mair, R.J., & Taylor, R.N. (1997). Bored tunnelling in the urban environment. In A.A. Balkema (Ed.), *Proceedings of the 14th International Conference on Soil Mechanics and Foundation Engineering, State-of-the-art Report and Theme Lecture* (Vol. 4, pp. 2353-2385). Balkema.

Möller, S., & Vermeer, P. (2006). Prediction of settlements and structural forces in linings due to tunnelling. In *Proceedings of the 5th International Conference of TC 28 of the ISSMGE* (pp. 621-627). The Netherlands, 15-17 june 2005.

Möller, S.C. (2006) *Tunnel induced settlements and structural forces in linings*. [Doctoral thesis, University of Stuttgard]. University of Stuttgard's repository. https://www.igs.uni-stuttgart.de/dokumente/Mitteilungen/54_Moeller.pdf

Ng, C.W.W., Lee, K.M., & Tang, D.K.W. (2004). Three-dimensional numerical investigations of new Austrian tunnelling method (NATM) twin tunnel interactions. *Canadian Geotechnical Journal*, 41(3), 523-539. http://dx.doi.org/10.1139/T04-008.

Nyren, R. (1998). *Field measurements above twin tunnels in London Clay*. [Doctoral thesis. Imperial College London]. Imperial College London's repository. https://spiral.imperial.ac.uk/handle/10044/1/8573

Ocak, I. (2014). A new approach for estimating of settlement curve for twin tunnels. In *Proceedings of the World Tunnel Congress'14*, Foz do Iguaçu, Brazil.

Peck, R.B., Hendron, A., & Mohraz, B. (1972). State of the art of soft-ground tunneling. In K.S. Lane & L.A. Garfield (Eds.), *Proceedings of the 1st Rapid Excavation and Tunnelling Conference* (Vol. 1, pp. 259–286). AIME.

Shivaei, S., Hataf, N., & Pirastehfar, K. (2020). 3D numerical investigation of the coupled interaction behavior between mechanized twin tunnels and groundwater – A case study: shiraz metro line 2. *Tunnelling and Underground Space Technology*, 103, 103458. https://doi.org/https://doi.org/10.1016/j.tust.2020.103458

Soliman, E., Duddeck, H., & Ahrens, H. (1993). Two- and three-dimensional analysis of closely spaced double-tube tunnels. *Tunnelling and Underground Space Technology*, 8(1), 13-18. http://dx.doi.org/10.1016/0886-7798(93)90130-N.

Sousa, J.N.V.A. (1998). *Túneis em maciços terrosos: comportamento e modelação numérica* [Doctoral thesis, University of Coimbra]. University of Coimbra's repository (in Portuguese). http://hdl.handle.net/10316/1874

Wan, M.S.P., Standing, J.R., Potts, D.M., & Burland, J.B. (2017). Measured short-term ground surface response to EPBM tunnelling in London Clay. *Geotechnique*, 67(5), 420-445. http://dx.doi.org/10.1680/jgeot.16.P.099.

Wu, B., & Lee, C. (2003). Ground movements and collapse mechanisms induced by tunneling in clayey soil. *International Journal of Physical Modelling in Geotechnics*, 3(4), 15-29. http://dx.doi.org/10.1680/ijpmg.2003.030402.